de Haas–van Alphen effect and the Fermi surface of LaB_6†

A. J. Arko, G. Crabtree, D. Karim, F. M. Mueller,* and L. R. Windmiller
Argonne National Laboratory, Argonne, Illinois 60439

J. B. Ketterson
Department of Physics, Northwestern University, Evanston, Illinois 60201
and Argonne National Laboratory, Argonne, Illinois 60439

Z. Fisk
Department of Physics, University of California, San Diego, La Jolla, California 92037
(Received 19 February 1976)

Extremal cross-sectional areas and effective masses of the Fermi surface of LaB_6 in the (100) and (110) planes have been measured using the de Haas–van Alphen (dHvA) effect. In addition, measurements of the field dependence of the magnetoresistance in the (100) plane have also been performed which show the existence of open orbits in certain directions and suggest the presence of magnetic breakdown. Much of the dHvA data are consistent with a set of nearly spherical ellipsoids located at the points X of the Brillouin zone and connected by necks which intersect the ΓM line; magnetic breakdown across the necks must be postulated to explain the remaining data. The proposed Fermi surface is consistent with the discrete variational band-structure calculations of Walch *et al.*

I. INTRODUCTION

The metal hexaborides of the type RB_6 form systems of considerable physical interest. These compounds are extremely hard, a fact that results from a strongly covalently bonded cage of boron atoms that surrounds the metal ion.[1] They are chemically and thermally quite stable. In addition the low work function of 2.7 eV makes them of potential interest as electron emitters. They may also have interesting superconducting properties. The crystal structure is simple cubic and is shown in Fig. 1.

The fact that these materials form with near perfect stoichiometry and are available with sufficient purity permits the fabrication of crystals with the relatively long low-temperature relaxation times required for de Haas–van Alphen (dHvA) or magnetoresistance studies of Fermi-surface properties. A preliminary account of our studies has appeared earlier[2,3]; an independent investigation has also been published recently.[4]

II. EXPERIMENT

A. Crystal preparation

The single crystals used in this investigation were grown at the University of California at La Jolla.[5] Lanthanum and boron in approximately the 1:6 atomic ratio were dissolved in an aluminum flux. The crucible, containing ~98% Al and 2% La-B mixture, was heated to approximately 1500 °C under an inert argon atmosphere in a resistance furnace. The temperature was then reduced at a rate of 25 °C/h to the solidification temperature by reducing the power. The aluminum was leached out using a saturated solution of sodium hydroxide leaving small faceted purple clusters of single crystals. These were separated into individual crystallites by treating with HNO_3. The single-crystal sample used in this investigation weighed ~200 μg and had a resistivity ratio of about 200. It has been reported that larger crystals with a comparable residual-resistivity ratio may be prepared using the floating zone technique under a pressurized argon atmosphere.[4]

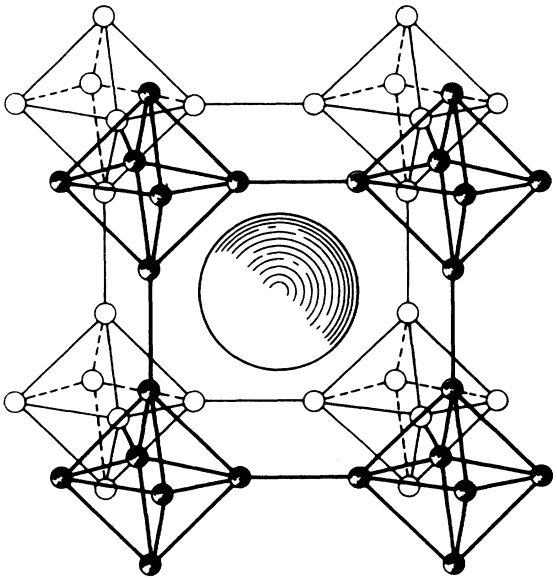

FIG. 1. Crystal structure of LaB_6.

B. Magnetoresistance measurements

Magnetoresistance data were obtained using the standard four-probe dc technique in a 75-kG superconducting solenoid at temperatures down to 1.2 °K. A rotating probe capable of two degrees of freedom[6] enabled us to obtain all the relevant information with one mounting of one specimen. The two degrees of freedom were achieved using a differential gear system. Potential leads can be spot-welded to LaB_6 if great caution is exercised. Most of our data were obtained using leads attached in this manner although conducting epoxy was also utilized. The geometry in the latter case is undesirable since one does not have point contacts on the potential leads and a relatively large Hall voltage can be measured together with the magnetoresistance.

C. dHvA spectrometers

A total of three dHvA spectrometer systems were used in this investigation. In all cases the large amplitude field modulation technique was employed.[7] The first system employed a 75-kG NbTi superconducting solenoid, and the sample was positioned with the same rotator used for the magnetoresistance measurements. The data for the (100) and (110) planes were taken in a single run. The sample was cooled using ^{4}He evaporative cooling to a minimum of 1.2 K. The initial runs showed that the dHvA spectrum contained a wealth of frequencies. Further data were taken in a second dHvA cryostat; coupled with this system was an on line PDP-11 minicomputer programmed to perform fast[8] and slow Fourier transforms.[9] Digitizing the data was accomplished using a Fabritek 1070 signal averager. This cryostat employed a NbZr-NbTi composite magnet with a maximum field of 72 kG and a homogeneity of five parts in 10^5 over a 1-cm-diam spherical volume. In this system the sample could be cooled to 1.1 or 0.4 °K using either ^{4}He or ^{3}He evaporative cooling. Precise vapor pressure thermometry was accomplished using a Texas Instruments precision pressure gauge. The lower temperatures were useful in enhancing the signal-to-noise ratio for the weaker signals. The one-degree-of-freedom sample rotator used has been described elsewhere[10]; the smooth action of this rotator permitted the taking of high-quality field rotation data. A final set of data were taken in a third system. This cryostat employed an Intermagnetics General 132-kG Nb_3Sn superconducting solenoid. The higher fields were useful for examining magnetic breakdown effects and revealed additional signals not seen in the other two systems. The sample could again be cooled with ^{4}He or ^{3}He and a high throughput pump system resulted in a minimum temperature of 0.30 °K (^{3}He). The one-degree-of-freedom sample rotator was of identical construction to that of the second system.

III. EXPERIMENTAL RESULTS

A. Magnetoresistance

Let us review briefly the qualitative features of Fermi surface topology which can be extracted from magnetoresistance data[11]: (i) If a metal is uncompensated (i.e., does not have an equal number of electrons and holes), and in addition possesses no open orbits (for the field direction under consideration), the high-field magnetoresistance $\Delta\rho/\rho_0$ saturates ($\Delta\rho = \rho(H) - \rho_0$); (ii) if the metal is compensated, and there is no open orbit, then one has $\Delta\rho/\rho_0 \propto H^2$. (iii) if we have open orbits then, if the open orbit direction (in k space) is not perpendicular to the current direction, $\hat{J}$, $\Delta\rho/\rho_0 \propto H^2$; if J is perpendicular to the open orbit direction, then $\Delta\rho/\rho_0$ saturates. Since magnetic breakdown can alter the nature of the orbits, high magnetic fields may cause a transition from one regime to another.

We now discuss the experimental results. For a general direction of H, saturation of $\Delta\rho/\rho_0$ is observed as H increases; thus we conclude that the metal is uncompensated (as expected from valence considerations). However, for $\hat{H} \perp [100] \parallel \hat{J}$ nonsaturating behavior was observed, characteristic of open orbits. Figure 2 shows a field rotation diagram of the magnetoresistance in the (100) plane for $\hat{J} \parallel [100]$ and for a field magnitude of $H = 62$ kG. For each direction of $\hat{H}$ in the (100) plane, the angle between $\hat{J}$ and $\hat{H}$ was varied through a small range centered nominally at 90°. The magnetoresistance is very sensitive to this angle, with a sharp maximum in $\Delta\rho/\rho_0$ for an angle of exactly 90°. These maximum values of $\Delta\rho/\rho_0$ are plotted in Fig. 2.

For directions other than $\hat{H} \parallel [100]$ or [011] we note a high magnetoresistance; magnetic field sweeps display the nonsaturating behavior characteristic of open orbits along the current direction (i.e., along [100]) for these intermediate directions. For $\hat{H} \parallel [001]$ or [011] the magnetoresistance tends toward saturation (but does not yet saturate at 65 kOe) indicating either (a) the lack of open orbits due to intersection, or (b) additional nonintersecting open orbits whose direction is perpendicular to $\hat{J}$. On the basis of the Fermi surface model to be introduced later case a and b may be true for $\hat{H} \parallel [001]$ and case b is true for $\hat{H} \parallel [011]$.

We point out that neither a true H^2 dependence nor saturation are observed at any orientation in the rotation diagram of Fig. 2. $\Delta\rho/\rho$ increases approximately as $H^{1.4}$ at the maxima and tends slowly toward saturation at the minima. Even at the maxima the exponent begins to decrease slightly

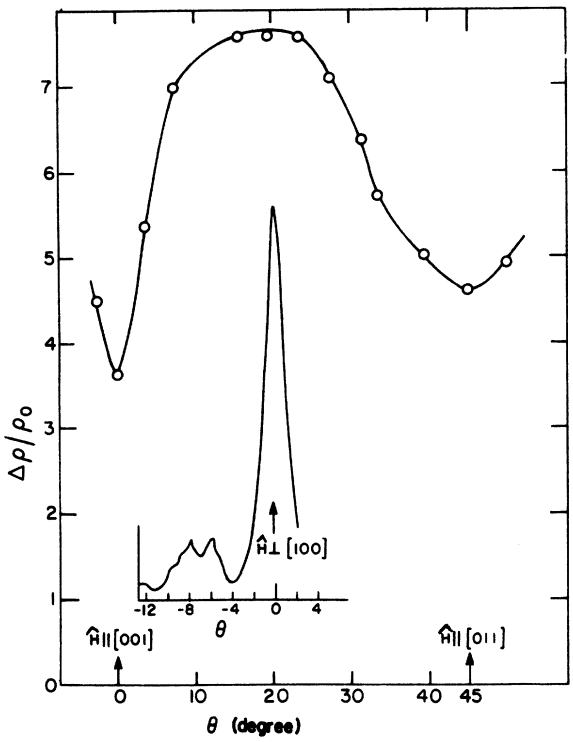

FIG. 2. Angular dependence of the magnetoresistance of LaB_6 for the field in a (100) plane with the current parallel to [100] and for a field of 62 kG. The inset shows a typical curve obtained if the sample is rotated through the point $\hat{H} \perp$ [100].

above ≈50 kG. We believe that this behavior is due to magnetic breakdown resulting in topological changes of the orbits. The relatively large $\Delta\rho/\rho_0$ (≈9 at 65 kG at the maxima) and the existence of well-defined oscillations (see below) tends to rule out the argument that $\omega_c\tau$ is less than 1. Furthermore, identical behavior was observed in a sample where $\Delta\rho/\rho_0 \cong 2$ at the maxima in a field of 65 kG.

More convincing evidence for magnetic breakdown can be seen in Fig. 3. Note the rather large amplitude low-frequency oscillations superimposed on the background magnetoresistance. Their frequency is nearly isotropic ($\approx 12\times10^{-5}$ a.u.) and they are observed at nearly all field directions where $\Delta\rho/\rho_0$ does not saturate. The number of carriers associated with such low frequencies would be expected to make a negligible perturbation on the magnetoresistance and the large amplitude observed is presumably due to breakdown between an open (or extended) orbit and a smaller piece in the vicinity of an interconnecting neck. Considerably weaker higher-frequency oscillations have also been observed at fields >50 kG. These are shown more clearly in the inset of Fig. 3 while the cross-sectional areas are shown as the solid triangles in Fig. 4. Clearly, magnetic breakdown appears to be associated with neck orbits (see below) and the frequency labeled $\chi_{2,3}$.

B. de Haas-van Alphen data

de Haas–van Alphen areas in atomic units versus magnetic field direction are shown in Fig. 4 for H in the (010) and (01$\bar{1}$) planes. Data with the 132-kG high-field system were taken only in the (01$\bar{1}$) plane. The area versus angle curves are very disjointed; none can be followed through the full range of angles studied.

It was possible in this material to observe up to six harmonics of each frequency even when the modulation amplitude was set to maximize the fundamental. Moreover, many combination frequencies of the type $f=(mf_1 \pm nf_2)$ were also observed indicating substantial magnetic interaction. Thus it was often difficult to determine which frequencies were fundamental, particularly where many frequencies were clustered. Some isolated frequencies shown in Fig. 4 may also be due to magnetic interaction but cannot be accounted for using the frequencies labeled in Fig. 4.

Figure 5 shows the symmetry points of the simple cubic Brillouin zone (BZ). We first focus our attention on the frequency branches marked χ_i in Fig. 4. We note that these frequencies are observed at almost all angles, there being two branches in the (01$\bar{1}$) and three in the (010) plane; we further note that the anisotropy is small, indicating a roughly spherical shape. The observed number of branches in each plane is consistent with a location of the "spheres" at the points X or M of the BZ; the point-group symmetry of these points is D_{4h} and the associated second-order sur-

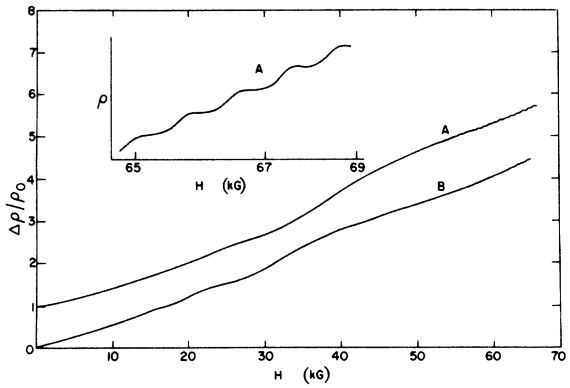

FIG. 3. Large amplitude oscillations in the magnetoresistance for $\hat{H}$ 5° from [110] (curve A) and $\hat{H}$ 5° from [100]. Note the faster oscillations at the highest fields (expanded view in inset).

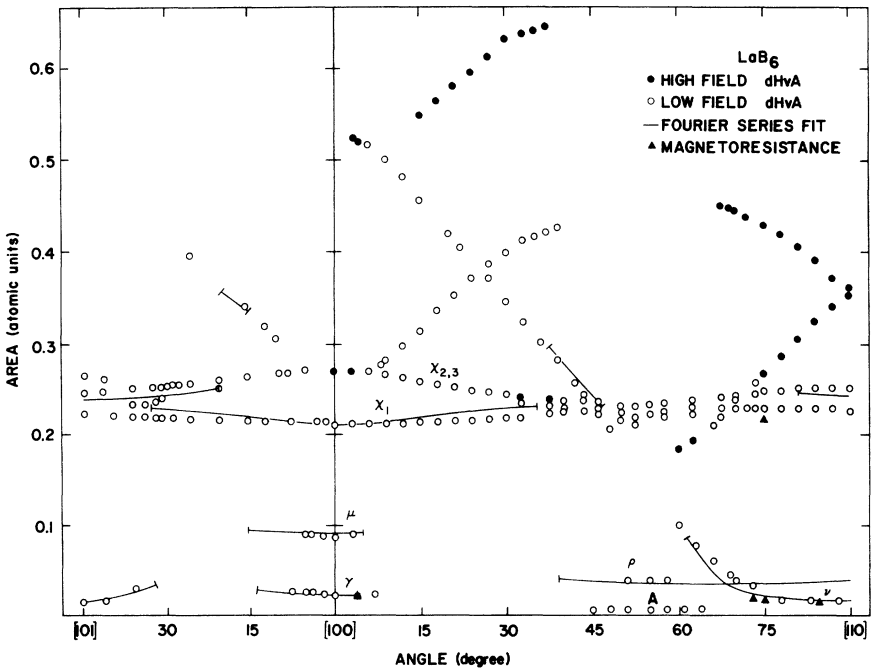

FIG. 4. Observed dHvA extremal areas in atomic units of the Fermi surface of LaB_6 for the magnetic field in the (100) and (110) planes. Solid points are high-field data, open circles are low-field data, and the solid lines are areas calculated from a Fourier series fit. No high-field data were taken in the (100) plane. Closed triangles indicate frequencies observed in the magnetoresistance.

face would be an ellipsoid of revolution. Since the band-structure calculations to be discussed in Sec. IV predict surfaces at the points X we will assume this location. We distinguish a principal ellipsoid (1) whose axis is along [100], the remaining two ellipsoids (2, 3) being designated as nonprincipal. As we tip the magnetic field away from [100] in a $(01\bar{1})$ plane, the frequencies of the nonprincipal ellipsoids are degenerate; for a general point in the (010) plane the frequencies of all three branches are nondegenerate. The frequency of the principal ellipsoid for $\hat{H} \| [100]$ is smallest; thus the axis of revolution of the ellipsoid ($X\Gamma$) is the long axis while the two XM axes are the short axes. At low fields the branches associated with the three ellipsoids could not be observed at all field angles. The solid points in Fig. 4 show the high-field data.

The majority of the observed dHvA data can be understood if it is assumed that the X centered spheres make contact with each other by necks extending along lines connecting the X points of the BZ. Such necks will intersect the ΓM symmetry direction and the band structure calculations along this line are consistent with this interpretation. Figure 5 also shows a schematic drawing of the proposed surface. The observation of the $\chi_{2,3}$ frequencies can be interpreted by invoking magnetic breakdown across the necks. This would be consistent with the magnetoresistance results. Here, however, a problem develops in making contact with the band structure calculations; while a multiply connected surface of the proposed type also follows from the band structure, a small magnetic breakdown energy through the necks is not expected.

Inspection of Fig. 5 shows that a number of additional extremal orbits are expected for a surface of this type and we will now discuss the remaining observed dHvA frequencies in terms of this model. For $\hat{H} \| [100]$ two small frequencies, γ and μ, are observed for only a limited range of angles. These are identified as four cornered rosettes with the γ orbit centered at Γ and the μ

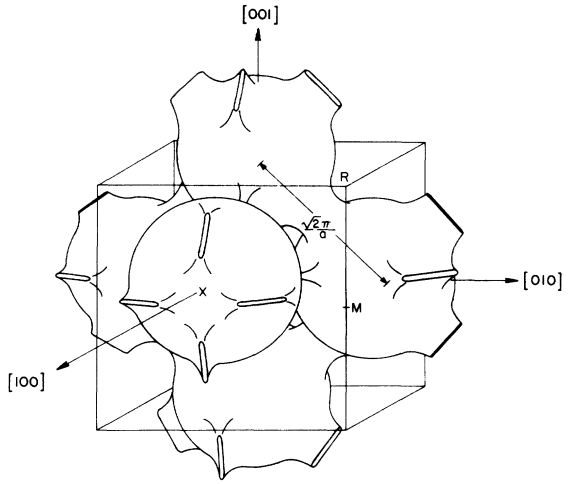

FIG. 5. Symmetry points of the simple cubic Brillouin zone and the proposed Fermi surface of LaB_6.

orbit centered at M. The ν orbit, which is observed for a range of angles for $\hat{H} \parallel [110]$, corresponds to extremal orbits around the interconnecting necks whose center lies on the ΓM line. The ρ orbit, which is observed for a range of angles around $\hat{H} \parallel [111]$, corresponds to a three cornered rosette whose center lies on the ΓR line.

The interpretation of the remaining dHvA frequencies is more tentative. We observe that the range of angles over which the neck orbit is observed appears to extend, with the exception of a break between about 30° to 45° from [110], to very near the [110] axis. The observation of this orbit over such a wide range of angles is not expected due to the presence of additional interconnecting necks and it is again necessary to invoke magnetic breakdown across such necks in order to explain these data; for $\hat{H} \parallel [100]$ an extrapolated "neck" area of approximately twice $\chi_{2,3}$ is expected and this is what is observed. There are four other branches with areas larger than 0.3 a.u. which are observed in the $(01\bar{1})$ plane. The largest of these has an area approaching that of the BZ face $[(2\pi/a)^2 = 0.641$ a.u.]. All of these are believed to be associated with orbits involving more than one ellipsoid and associated interconnecting necks. Since the (010) plane was not run in the 132-kG system, the behavior of these or similar branches in that plane is not known. Two branches, which are degenerate at [110], are observed to split on rotating the sample away from this direction; since neither of these branches has a turning point at [110], these orbits cannot be centered on a symmetry point. For $\hat{H} \parallel [110]$, extremal orbits about two of the 12 necks that reside in the first BZ are associated with the minimum neck area ν and two more are associated with open orbits; orbits centered on the eight remaining necks are believed to be responsible for the unexplained branches and these would split into two groups of four (one group with increasing and the other with decreasing area) as the field is rotated away from [110] in the $(01\bar{1})$ plane. It may again be necessary to invoke magnetic breakdown to account for the existence of these orbits at some angles. Two remaining branches are observed for a range of magnetic field angles in the $(01\bar{1})$ plane; the precise nature of these orbits is not understood; the larger one presumably involves three ellipsoids. For the field in the (010) plane (where the cryostat involving the 72-kG system was used) only one area larger than 0.3 a.u. was observed and this one involves the two ellipsoids responsible for the χ_1 and χ_2 frequencies.

We have at present no explanations for the relatively strong frequency labeled A in Fig. 4. We do not totally discount the possibility of having misassigned the three-cornered rosette orbit presently labeled ρ, although this seems unlikely in view of the fit obtained in the Fourier series fit to the data.

TABLE I. Effective mass data on LaB_6 in (110) plane.

Branch	Angle from [100] (deg)	mass m^* Experimental	mass m^* Band structure $\alpha = 0.7$
A	54.7	0.234	
ν	71	1.14	
ν	90	0.460	
χ_1	0	0.610	0.40
χ_1	37	0.642	
χ_1	90	0.650	
$\chi_{2,3}$	90	0.650	
γ	0		0.37
μ	0		0.61

At very low magnetic fields (less than 10 kG), an approximately isotropic extremal area of $10 \pm 3 \times 10^{-5}$ a.u. was observed. The field sweeps contained beats and thus the location of the orbit must be other than Γ or R. The dominant low frequency oscillations observed in the magnetoresistance may well be associated with these extremal areas. If so, magnetic breakdown across the necks may occur via these small pieces of the Fermi surface. The residual field (resulting in poor field calibration), the beats, the limited number of oscillations and required modulation amplitudes beyond the capability of our equipment prohibited a detailed amplitude study of this frequency. We believe, however, that its amplitude decreases faster at high fields than expected simply from Bessel-function considerations.

Effective masses were measured from the temperature dependence of the dHvA amplitude. Data were taken between 1 and 2 °K using ^{4}He evaporative cooling in fields as large as 50 kG. Because the frequency branches are so closely spaced, mass measurements were possible at only a few angles. The results are summarized in Table I. The mass of the branch χ_1 is very flat over the entire (110) plane. The masses of χ_2 and χ_3 are identical with that of χ_1 at [100], supporting the argument that these branches are related by symmetry. The mass of the ν branch varies appreciably, rising by over a factor of 2 between [110] and the angle at which it first disappears. The band-structure calculations of masses (described in Sec. IV) can be compared with experiment at only one angle as shown in Table I. The large enhancement inferred from the comparison has been discussed earlier from the point of view of the electron-phonon interaction.[3]

Magnetic breakdown is required for the dHvA data to be consistent with the model of Fig. 5. In particular, the existence of the branches χ_2, χ_3

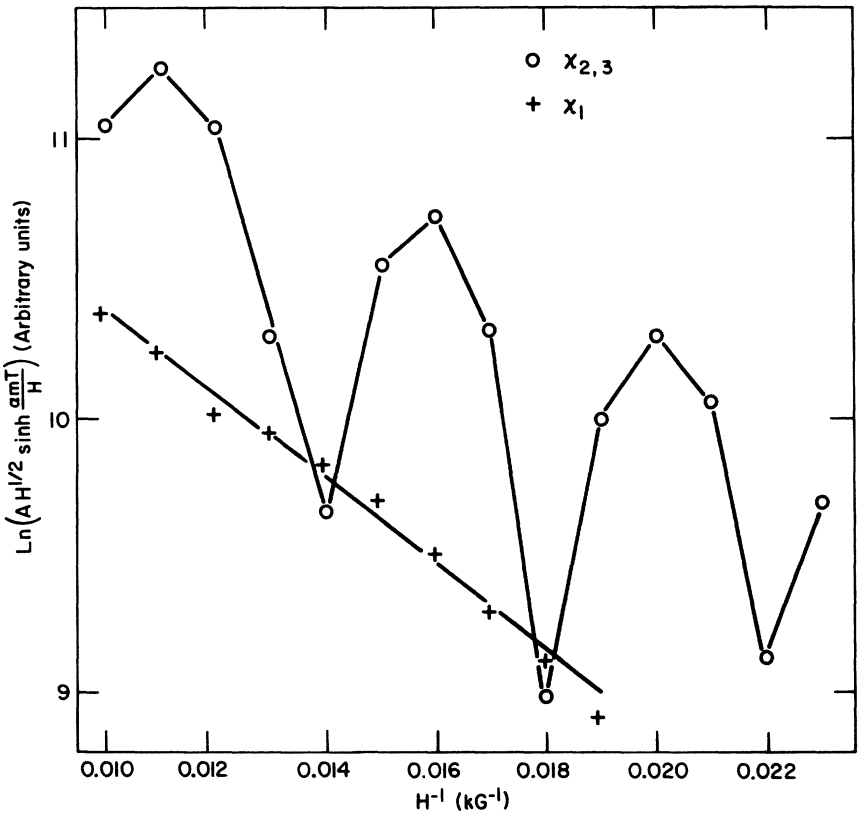

FIG. 6. Dingle plot at 88° from [100]). The straight line through the χ_1 data is a least-square fit to the points.

in the (110) plane must result from breakdown across the necks; otherwise these orbits would be open for a general angle in the (100) plane. The magnetoresistance data show evidence for breakdown and indicate the involvement of the necks in the breakdown process. Magnetoresistance cannot take us beyond this step. The field dependence of the dHvA amplitude is also sensitive to breakdown, and attempts were made to verify breakdown for the $\chi_{2,3}$ branch (observed at one angle in magnetoresistance) at several angles in the (110) plane. "Dingle plots" of $\ln[AH^{1/2}\sinh(\alpha mT/H)]$ vs $1/H$ were made at 14°, 18°, 65°, 75°, and 88° from [100] in the (110) plane, where A is the observed dHvA amplitude, m is the cyclotron effective mass (assumed to be 0.60 for all orientations), $\alpha = 146.9$ kG/K, and H and T are the field and temperature. In the absence of magnetic breakdown such a plot is a straight line with slope $-\alpha mX$, where X is the Dingle temperature. For an orbit which exists through breakdown, such as $\chi_{2,3}$, the amplitude should rise much faster than normal as a function of field as more and more electrons contribute to the orbit, and the Dingle plot may show curvature. In the case of $\chi_{2,3}$, the situation is further complicated by the double degeneracy of the breakdown orbits. This causes oscillations or beats on the Dingle plot, because the experimental field direction could not be oriented precisely in the (110) plane.

A Dingle plot for $\hat{H}$ 88° from [100] is shown in Fig. 6. The upper curve is the amplitude of $\chi_{2,3}$ and the lower that of χ_1. Assuming the beats are due to degeneracy (there may be alternative explanations since the beats were curiously insensitive to misorientation out of the plane) the overall rate of increase for $\chi_{2,3}$ is about the same as for χ_1. Therefore if any breakdown occurs at this orientation, it must take place at such low fields that the breakdown is complete at the smallest field represented on the Dingle plot (43 kG). Below this field the signal is too weak to observe. Three of the other Dingle plots also show $\chi_{2,3}$ rising about as fast as χ_1. The plot for $\hat{H}$ 14° from [100] shows $\chi_{2,3}$ rising noticeably faster than χ_1. Therefore we conclude that if breakdown is responsible for the $\chi_{2,3}$ branch, the breakdown field is very small but may increase somewhat for $\hat{H}$ near [100]. This latter orientation corresponds to breakdown through the thick part of the necks.

dHvA data in LaB_6 have been recently reported by Ishizawa *et al.*[4] Most of their data pertains to the χ frequencies (α in their notation). The maximum field available in their investigation was 60 kG and their angular range of observation of the

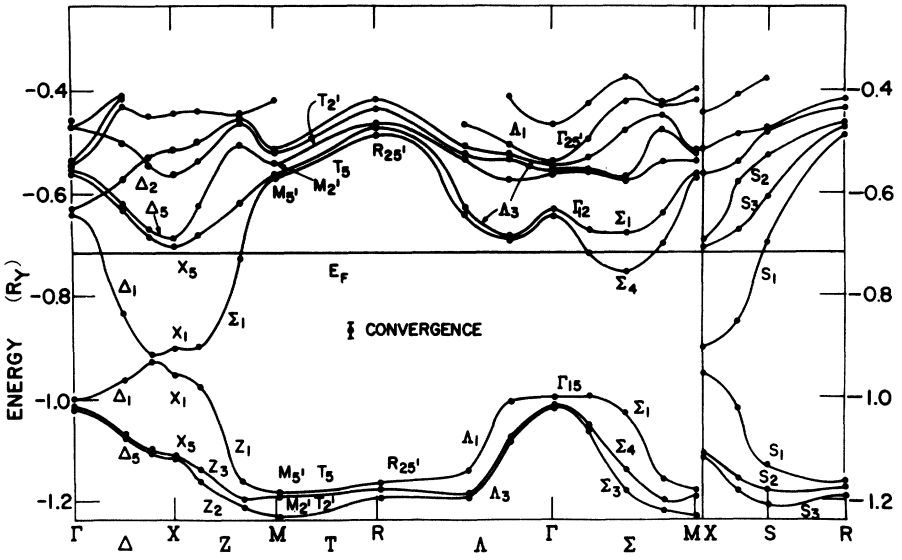

FIG. 7. Band structure of LaB_6 for $\alpha = 1$.

$\chi(\alpha)$ frequencies was smaller than ours. They have also interpreted their data by introducing interconnecting necks among the ellipsoids in order to explain additional orbits and the absence of dHvA frequencies at certain angles.

IV. BAND-STRUCTURE CALCULATIONS

Two band structures for LaB_6 were calculated by Walch *et al.*[3,12] Both use the discrete variational method which allows the inclusion of non-muffin-tin potentials which are inherent in LaB_6. The calculations were performed with ground-state neutral atom configurations and exchange parameters $\alpha = 0.7$ and 1.0. The band structures do not differ significantly in their essential features. The $\alpha = 1.0$ calculations are shown in Fig. 7. The Fermi energy was located by fitting the energy bands to a symmetrized Fourier series[12] from which a density of states histogram was computed. Note that the Fermi energy E_F cuts only a single level. Focusing our attention on the structure near X we note that there is an electron surface centered at X which is closed along the $X\Gamma$ (Δ_1) and XM (Z_1) directions. We also note that the Σ_4 level intersects the Fermi energy in the ΓM direction; this is just what is required if there are to be necks connecting the X centered ellipsoids.

Extremal areas calculated from the Fourier series fit to the $\alpha = 0.7$ bands are shown in Table II, together with the experimental areas for symmetry directions. Reference to Fig. 7 shows that the agreement could be improved if the Fermi level is raised slightly. Effective masses were obtained from area calculations for the energies -0.280 and -0.290 hartree, where $E_F = -0.285$ hartree (1 hartree = 27.2 eV). These masses are shown in Table I with the experimental masses.

Preliminary orbit tracing calculations were carried out using the 11 term Fourier series fit to the $\alpha = 1$ band structure calculations for the level cutting E_F (the 44th band including spin degeneracy); these calculations verified that the Fermi surface was generally of the proposed shape and connectivity. The coefficients in the Fourier series were then varied to fit selected experimen-

TABLE II. Area data for LaB_6 in (110) plane.

Branch	Angle from [100] (deg)	Area (a.u.) Experimental	Band structure $\alpha = 0.7$
χ_1	0	0.211	0.15
γ	0	0.023	0.060
μ	0	0.086	0.12
ρ	54.7	0.025	
ν	90	0.015	

TABLE III. Coefficients of the stars in the Fourier series fitted to the experimental data.

Star	Coefficient
0	0.00451
1	−0.01744
2	0.00816
3	0.00633
4	−0.00209
5	−0.00140
6	−0.00072
7	0.00038
8	−0.00082
9	0.00205
10	−0.00112

tal data. The solid lines in Fig. 4 show the resulting areas. It will be observed that the experimental data are usually observed over a wider range of angles than is expected from the calculations. One might say that the increased observational range is due to magnetic breakdown; however the gap associated with Σ_4 level would be expected to be far too large to be bridged by the fields available in the present experiment. We offer no resolution for this dilemma; it could be that the agreement with the band structure calculations is fortuitous. The coefficients of the stars in the Fourier series fitted to the experimental data are contained in Table III. Some caution is required in the use of this Fourier series representation as multiple solutions exist at certain angles.

Recently, Perkins, Armstrong, and Breeze[14] have calculated the band structure of several metal hexaborides by a linear-combination-of-atomic-orbitals method. The Fermi surface they deduce for LaB_6 consists of three sheets: two closed pieces centered at Γ and a multiply connected "jungle gym" of cylinders running along [100] and meeting at Γ. The dHvA data we report here cannot be interpreted on the basis of this model.

---

†Based on work performed under the auspices of the U.S. Energy Research and Development Administration.

*Present address: Fysisch Laboratorium Faculteit der Wiskunde, En Natuurwetenschappen, Katholieke Universiteit, Driehuizuizerweg 200, Nijmegen, Nederland.

[1]L. Pauling, *The Nature of the Chemical Bond* (Cornell U.P., Ithaca, N.Y., 1960); *The Chemistry of Boron and Its Compounds*, edited by E. L. Muetterties (Wiley, New York, 1967); H. J. Goldschmidt, *Interstitial Alloys* (Butterworth, London, 1967), Chap. 6.

[2]A. J. Arko, G. Crabtree, J. B. Ketterson, F. M. Mueller, and L. R. Windmiller, Bull. Am. Phys. Soc. 19, 250 (1974).

[3]A. J. Arko, G. Crabtree, J. B. Ketterson, F. M. Mueller, P. F. Walch, L. R. Windmiller, Z. Fisk, R. F. Hoyt, A. C. Mota, R. Viswanathan, D. E. Ellis, A. J. Freeman, and J. Rath, Int. J. Quant. Chem. S 9, 569 (1975).

[4]Y. Ishizawa, S. Kawai, and E. Bonnai, *Proceedings of the Fourteenth International Conference on Low Temperature Physics* (Helsinki University P., Helsinki, 1975).

[5]Z. Fisk, A. S. Copper, P. H. Schmidt, and R. N. Castellano, Mat. Res. Bull. 7, 285 (1972).

[6]G. F. Brennert, W. A. Reed, and E. Fawcett, Rev. Sci. Instrum. 36, 1267 (1965).

[7]R. W. Stark and L. R. Windmiller, Cryogenics 8, 272 (1968).

[8]L. R. Windmiller, J. B. Ketterson, and J. C. Shaw, ANL-7907 available through National Technical Information Service, U. S. Dept. of Commerce (1972) (unpublished).

[9]G. W. Crabtree, thesis (University of Illinois of Chicago Circle, 1974) Available from University Microfilms, Ann Arbor, Mich. (unpublished).

[10]L. R. Windmiller and J. B. Ketterson, Rev. Sci. Instrum. 39, 1672 (1968).

[11]A. B. Pippard, *The Dynamics of Conduction Electrons* (Gordon and Breach, New York, 1965).

[12]P. F. Walch, D. E. Ellis, and F. M. Mueller (unpublished).

[13]J. B. Ketterson, F. M. Mueller, and L. R. Windmiller, Phys. Rev. 186, 656 (1969).

[14]P. G. Perkins, D. R. Armstrong, and A. Breeze, J. Phys. C 8, 3558 (1975).